Investigation of mass-TKE distributions of fission fragments from the ^{235}U(n,f)-reaction in resonances

Shakir ZEYNALOV, Walter FURMAN
Joint Institute for Nuclear Research, Frank Lab. of Neutron Physics, Russia

Franz-Josef HAMBSCH
EC-JRC-Institute for Reference Materials and Measurements, Belgium

Resonance neutron induced fission fragment properties were studied in the incident neutron energy range from thermal up to 35 eV. The pre-neutron emission mass and kinetic energy distributions have been measured with a Frisch-gridded double ionisation chamber. The two-dimensional mass-TKE distributions for low energy resonances have been described in terms of fission modes and compared with theoretical calculations in the frame of the multi-modal random neck-rupture model. Variation of the fission modes obtained in Ref. [1] as well as the scale of the fluctuation of fission mode weights in different neutron resonances (~15% for standard I and ~4% for standard II) have been confirmed by our measurements.

KEYWORDS: NUCLEAR REACTIONS: ^{235}U(n,f), Mass-energy distributions, Mean total kinetic energy vs E_n, Multi-modal random neck-rupture model

I. Introduction

The aim of the present work was to obtain experimental data on the incident neutron energy dependence of the relative weights of the two main asymmetric fission modes, which make up the mass distribution of the ^{235}U(n,f)-reaction. This dependence of the fission modes as a function of incident neutron energy in ^{235}U(n,f) was discovered in Ref. [1]. But so far it is the only measurement where fission mode fluctuations in resonance neutron induced fission were detected and the statistical significance of the data of Ref. [1] below 8 eV was not high enough to make conclusions on the scale of the fluctuations. Measurements of fission fragment (FF) mass and total kinetic energy (TKE) distributions of ^{235}U(n,f) were carried out at the Dubna IBR-30 time of flight spectrometer in the resonance neutron energy range from thermal up to 35 eV. In the energy range from thermal to 8.77 eV individual resonances could be resolved, but for the higher incident neutron energies the resolution degraded due to the rather large (4 μs) width of the neutron pulse. Although the fission mode fluctuations which were found in Ref. [2] revealed similar incident neutron energy dependence as was observed in Ref. [1], the scale of the fluctuations and the shape was slightly different. Based on the progress in fission cross-section and the multi-modal model calculations reported in Ref. [3] it was found reasonable to reanalyse the data of the measurement reported earlier in Ref. [2] to find out the possible cause of the difference in results.

The data analysis was carried out in two steps. At first step the data acquisition apparatus was investigated on the influence of the neutron source flash to the precision of the fission fragment TKE measurements. Necessary improvements and careful adjustment of the base line restorer circuitry of the spectroscopic amplifier were made before the measurement was launched. Finally FF mass yield and TKE distributions were determined for various incident neutron energy intervals and the difference of these values obtained for thermal and

resonance neutron energies was constructed. In contrast to Ref. [1] we realised true relative measurements (with respect to thermal energy). The data analysis confirmed the main characteristics of the asymmetric fission modes obtained in Ref. [1] from thermal neutron

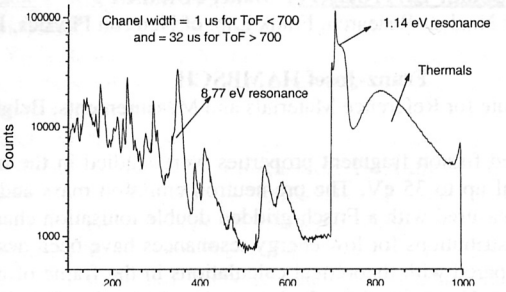

Fig.1 Fission events TOF distribution

induced fission of ^{235}U as well as the scale of the fluctuation of the fission mode weights in different neutron resonances (~15% for the standard I and ~4% for the standard II mode). Some differences between the results of the present work to the results obtained in Ref. [1] could be explained by the worse neutron energy resolution of the present investigation as well as due to the data analysis, where new calibration results obtained after the publication of Ref. [1] were used.

II. Neutron source

The IBR-30 reactor was used as a pulsed neutron source with close to 100 Hz pulse repetition frequency and 9.8 kW beam power. The pulse structure of the neutron source is rather complicated and can be considered for simplicity as the superposition of three neutron sources with an integral flux of $3*10^{16}$ neutrons per second. The neutron source components

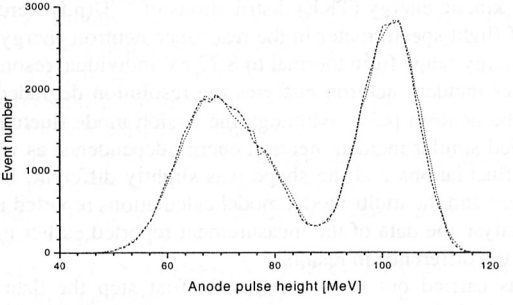

Fig.2. Comparison of the kinetic energy distributions of the sample side (dotted line) and the backing side (dashed line) at thermal energy after applying the necessary corrections.

are a steady state reactor flux plus two synchronously pulsed sources with a full width at half

maximum (FWHM) of ~800 μs and ~4 μs respectively. The steady state part of the reactor neutrons was used for continuous monitoring of the stability of the apparatus during the measurements in the following way. Fission events located between resonances in the TOF spectrum (see Fig. 1) caused mainly by the steady state component of the neutron flux. Their TKE distribution should be independent on TOF.

Usually 12 such intervals located in the dips between resonances with neutron energies from thermal up to 35 eV were chosen. The quality of the base line restorer of the spectroscopy amplifier was accepted as satisfactory if the scattering of TKE values obtained for different intervals was inside a 0.1 MeV margin during the whole measurement. That principle provided us assurance of the consistency of the obtained experimental data in the incident neutron energy range below 35 eV. At higher incident neutron energies the stability of the apparatus was not good enough to perform a data analysis with acceptable quality. As was mentioned above the results of our previous measurements reported in Ref. [2] were slightly different from those reported in Ref. [1]. The reason of such a difference was found after the reanalysis of the data using the above described principle of the spectroscopy amplifier quality monitoring.

The pulsed source with the narrower neutron pulse was used for the resonance neutron induced fission investigations using the TOF technique, but the pulsed source with the wide pulse produces a so-called low resolution TOF spectrum which has the same nature as the high resolution one. As a result of the interference of the two TOF distributions the final TOF spectrum should be considered as a superposition of two TOF spectra. The overlapping of resonance peaks caused by the wider pulses in the TOF distribution lead to an up-rising tail for the higher energy neutrons (lower TOF) as can be seen in Fig. 1.

III. Experimental setup and data analysis

The neutron beam from the IBR-30 reactor source was tailored by a collimator system to a diameter of 5 cm on the target position. The uranium sample with a thickness of ~60 $\mu g/cm^2$ was vacuum evaporated on a polyimide layer of 33±3 $\mu g/cm^2$ and covered with a gold layer of ~20$\mu g/cm^2$. The target was mounted on the common cathode of a double Frisch-gridded ionization chamber. The anodes were made of stainless steel plates with a diameter of 150 mm. The grids were made of copper wires of diameter 0.1 mm stretched over an annular steel ring with inner and outer diameter of 130 mm and 150 mm, respectively. The grid wire spacing was 2 mm and the grid-anode and grid-cathode distance was 10 and 27 mm, respectively. The chamber was operated with a 90%Ar+10%CH_4 (P-10) gas mixture at a constant pressure of 1.05 bar. Normally the working gas was refreshed periodically every 24 hour during the 10 days of the reactor run, but there were runs without working gas refreshment during five days. The latter measurement was done for working gas degradation tracking.

Data analysis was performed taking into account the Frisch-grid inefficiency (as defined in Ref. [4]), the energy loss in the target as well as in the backing, the pulse height defect in the counter gas and momentum conservation laws. After having applied all the mentioned corrections to the raw anode and sum pulse height signals, a quality check has been made by comparing the corrected anode signals of both sections of the chamber. The quality of the data reduction procedure could be tested by comparison of the kinetic energy distributions for both sections of the chamber as shown in Fig. 2.

In our approach we used the relative measurement procedure based on the simultaneous measurement of fission fragment characteristics for thermal and resonance neutron induced fission. For this reason a small hole was drilled in the center of the Cd filter placed between the exit of the neutron beam tube and the ionization chamber. It was made to allow a small part of thermal neutrons to reach the target bypassing the Cd filter. Thermal neutron induced fission was separated from resonance neutron induced fission by time-of-flight and was used as a reference (see Fig. 1). Fission fragment energies were derived from the pulse height data after the above mentioned corrections using the formula:

$$E_i = A_i + B_i \times P_A^i + PHD(E,A)$$

The calibration parameters needed to construct the absolute energy scale were evaluated from the thermal neutron induced fission pulse height distributions. We used the mean of the light FF kinetic energy and TKE values from literature [5]. In the above formula PHD(E,A) represents the pulse height defect which we calculated in LSS units as proposed in Ref. [6].

With the laws for momentum and mass conservation and the measured two fragment kinetic energies the masses of both fragments were calculated using the procedure described in Refs. [1,7]. Thus for each incident neutron energy range covering neutron resonance areas from thermal up to 35 eV two-dimensional arrays in mass-TKE coordinates have been obtained. In Fig. 3 the mass yield curve obtained in this work is compared with the mass yield curve from Ref. [5].

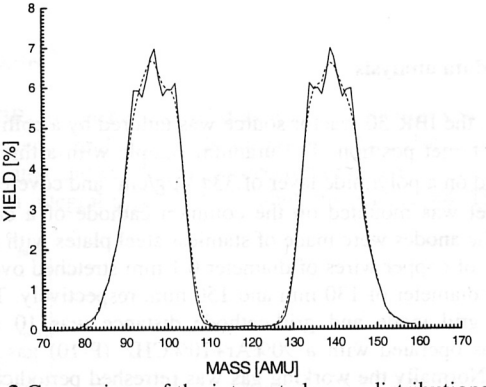

Fig. 3 Comparison of the integrated mass distributions of the present work (dashed line) and from Ref. [5] (solid line).

The differences between resonance and thermal neutron induced fission yields have been plotted in Fig. 4 for the present measurement. By comparison of the mass yield differences obtained in this work with that obtained in Ref. [1], we verified a good qualitative and quantitative agreement between both investigations despite of the difference between neutron sources, measurement and data analysis procedures.

The two-dimensional Y(A,TKE) distribution is commonly used for comparison with model calculations. One of the widely used models in low energy fission studies is the multi-modal random neck-rupture model (MM-RNR) of Brosa et al. [8], because it provides not only a qualitative but also quantitative description of the fission process. The existence of several modes in the potential energy landscape, leading to different scission shapes of the compound system is commonly accepted. For ^{235}U fission the MM-RNR model predicts two standard asymmetric modes and one symmetric mode, so called S1 (Standard 1), S2 (Standard

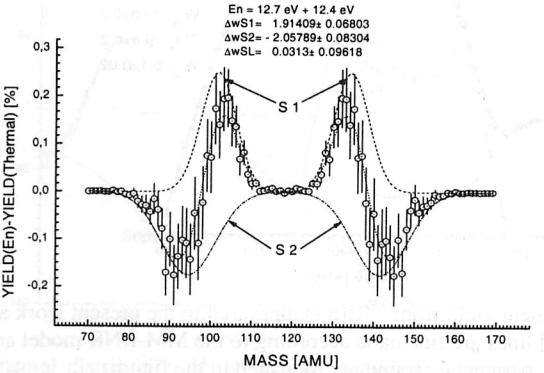

Fig. 4 Fission fragment yield difference for a given resonance group (indicated on the figure) with respect to the thermal values.

2) and SL (Super long). The experimentally measured Y(A,TKE) distribution can be understood as a superposition of the individual mass and TKE distributions of the different modes. The fit of the two-dimensional mass-TKE distribution has been performed to obtain an energy dependence of the fission mode distribution. A E_n dependence of the fission mode contributions is not considered in the
frame of the MM-RNR model. But until now that model is the only one that provides a good tool to parameterise the two-dimensional mass-TKE distribution and thus allows a quantitative comparison of the measured parameters. The parameterisation proposed by Brosa and Knitter [9] was used to decompose the Y(A,TKE) distribution at each investigated incoming neutron energy. It includes three modes with energy-dependent average mass and mass dispersion and energy dependent TKE and σ_{TKE}. The difference in the mass yield data was also decomposed into three (S1 –dashed line and S2- dash-dotted line, SL – not shown) fission modes and plotted for reference in Fig. 4 along with the resulting curve (doted line). The MM-RNR model parameters for the thermal neutron energy were found by fitting of the experimental data measured at thermal energy as shown in Fig. 5. The following equation was used in the fit :

$$Y(A)=\frac{W_{S1}}{\sigma_{S1}^2\sqrt{2\pi}}\exp\left(-\frac{(A-A_{S1})^2}{2\sigma_{S1}^2}\right)+\frac{W_{S2}}{\sigma_{S2}^2\sqrt{2\pi}}\exp\left(-\frac{(A-A_{S2})^2}{2\sigma_{S2}^2}\right)+\frac{2*W_{SL}}{\sigma_{SL}^2\sqrt{2\pi}}\exp\left(-\frac{(A-118)^2}{2\sigma_{SL}^2}\right) \quad (1),$$

The A_i ,W_i , σ_i being the mean mass number, weight and dispersion, were found as fitting parameters for the S1,S2 and SL fission modes, respectively. The final result of the

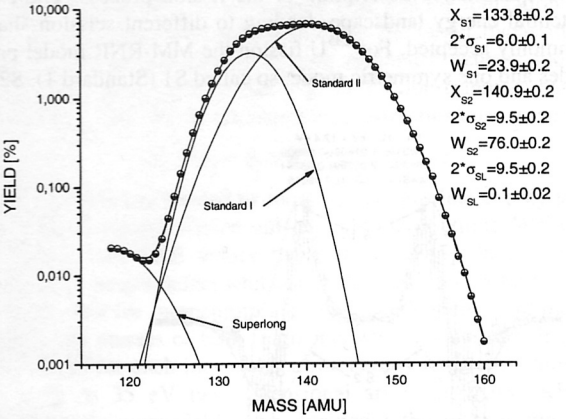

Fig. 5 Fission fragment yield from ^{235}U(n,f) measured in the present work at thermal energy. The full lines are fits made according to the MM-RNR model and the parameters found are indicated in the figure.

described fitting procedure is presented in Table I and were used as a reference for the calculation of the resonance neutron induced fission mode fluctuation as in Ref. [1].

Table I. MM-RNR model parameters were found as fitting parameters of experimental data

Mode	Wi	Mi	$2*\sigma_{Mi}$	D_i	TKE_{bar}
S1	16.2±0.5 (15.2±0.6)	133.8±0.2 (133.8±0)	5.2±0.1 (4.8±0.1)	16.1±0.1 (16.0±0.1)	186±0.6 (186±1)
S2	83.9±0.6 (84.4±0.9)	141.1±0.2 (141.1±01)	9.9±0.1 (10.1±0.1)	17.3±0.1 (17.5±0.1)	171±0.6 167±1)
SL	0.10±0.02 (0.069±0.001)	118	10.1±0.0 (10.1±0)	18.5±0.2 (19.4±0.1)	163±5 (157±7)

The values of A_i ,W_i , σ_i found for fission modes at thermal energies were used to perform the fits of the fission fragment yield difference at selected resonance neutron energies in respect to the thermal values similar to that shown in Fig. 4. The results of the fission mode fluctuations expressed as the difference of weights of fission modes are presented in Table II. The fission mode parameters obtained as described above were used to make a fits of the averaged total kinetic energy TKE(A) as a function of the mass split for the Y(A,TKE) distribution measured at resonance energies. These fits were made using the following equation taken from Ref. [8]:

$$Y(TKE,A) = (\frac{200}{TKE})^2 h \exp(\frac{-(L-L_{max})^2}{(L-L_{min})l_{dec}}), \text{ where } L = \frac{1.44Z(Z-Z_{cn})}{TKE} \quad (2)$$

TKE stands for total kinetic energy of the fragments, L is the distance between charge centers of the fragments, L_{max} is the distance between fragment charges at which the distribution reaches its maximum, L_{min} is the minimum possible distance between fragments, l_{dec} – is the distribution shape factor, Z is the electric charge of the fragment and h is a parameter defining the height of the distribution.

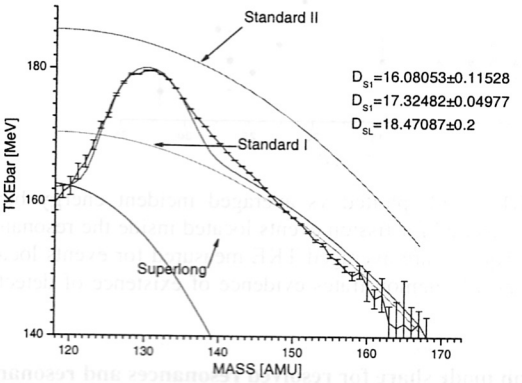

Fig. 6 Experimental distribution of the average total kinetic energy TKE_{bar} vs fragment mass for thermal neutron energies. The fit made using the MM-RNR model is obtained as supersion modes

Results of the fit are presented in Fig. 6, where the experimental data obtained at thermal neutron energies were fitted using equation (2) for Y(TKE,A) and data for the fission mode contributions obtained for mass distributions as presented in Fig. 5. The solid curves in Fig. 6 labeled as Standard I, Standard II and Superlong correspond to the average total kinetic energy versus mass value dependence for the corresponding fission mode. These dependencies along with the fission mode shares W_i were used to plot the final curve for the comparison with experimental data as shown in Fig. 7. A similar procedure was applied to each resolved resonance neutron energy interval. The resonance neutron energy group (12.7 eV+ 12.4 eV) could not be resolved in the present measurement, but the data were analyzed for reference because at that energy range the difference in respect to thermal neutron energies reaches a local maximum and the statistics acquired is very good. Results of resonance neutron energy dependence on the fission mode shares are summarized in Table II.

That presentation was proposed in Ref. [8] and provides better agreement with experimental data, but implementation for two dimensional MASS&TKE distribution fitting meets much more technical difficulties. The representation used in the present work provides better agreement with experimental data as compared to Ref. [1]. All differences in the fission mode values between the present work and Ref. [1] are within the measurement errors and could be explained by the difference in the calibration procedure and the reference data for the mass distribution. Finally in Fig.7 the incident neutron energy dependence of the average TKE for FF is plotted, which demonstrates a clear evidence of the existence of differences between resonance and thermal neutron induced fission of ^{235}U.

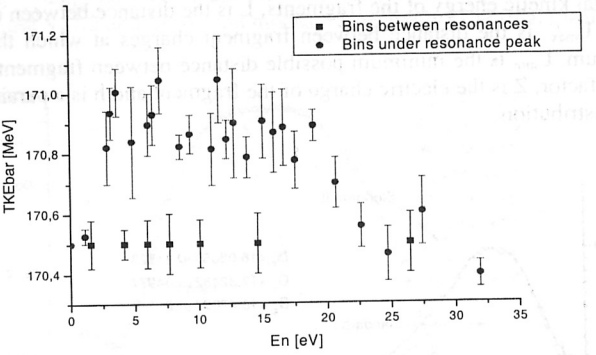

Fig. 7 Average TKE of FF plotted vs averaged incident energy bins. The circles represent the TKE measured for fission events located inside the resonance peaks in the TOF spectrum. The squares are averaged TKE measured for events located in between resonance peaks. It clearly demonstrates evidence of existence of detectable variations in TKE

Table II. Fission mode share for resolved resonances and resonance groups

E_n [eV]	W_{S1}	W_{S2}	$2*W_{SL}$	W_{S1}/W_{S2}
12.4+12.7	18.10±0.4 (1.9±0.1)	81.80±0.6 (-2.1±0.1)	0.23±0.1 (0±0.1)	0.27±0.02
11.67	18.20±0.4 (2.0±0.2)	81.60±0.6 (-2.3±0.2)	0.34±0.2 (0.1±0.2)	0.27±0.02
10.18	17.80±0.4 (1.6±0.1)	82.30±0.6 (-1.6±0.1)	0.2±0.1 (0±0.2)	0.27±0.02
9.28	17.30±0.4 (1.1±0.1)	82.80±0.6 (-1.1±0.1)	0.36±0.1 (0.2±0.1)	0.26±0.02
8.77	17.20±0.4 (1.0±0.05)	82.80±0.6 (-1.1±0.05)	0.2±0.1 (0.0±0.1)	0.26±0.02
7.08	18.30±0.4 (2.1±0.1)	81.60±0.6 (-2.3±0.1)	0.26±0.1 (0.1±0.1)	0.27±0.02
6.38	18.50±0.4 (1.3±0.1)	82.50±0.6 (-1.4±0.1)	0.32±0.2 (0.1±0.1)	0.26±0.02
6.10	18.60±0.4 (1.4±0.1)	82.40±0.6 (-1.5±0.1)	0.22±0.2 (0±0.2)	0.26±0.02
5.20	16.70±0.4 (0.5±0.2)	83.40±0.6 (-0.5±0.2)	0.20±0.2 (0±0.2)	0.24±0.02
4.85	18.60±0.4 (1.2±0.1)	82.60±0.6 (-1.3±0.1)	0.20±0.1 (0±0.2)	0.26±0.02
3.61	16.20±0.4 (0±0.1)	83.90±0.6 (0±0.1)	0.20±.0.1 (0±0.2)	0.24±0.02
3.14	16.20±0.4 (0±0.1)	83.90±0.6 (0±0.1)	0.20±.0.1 (0±0.2)	0.24±0.02
1.14	16.20±0.4 (0±0.1)	83.90±0.6 (0±0.1)	0.20±.0.1 (0±0.2)	0.24±0.02
Thermal	16.20±0.4	83.90±0.6	0.20±.0.1 (0±0.2)	0.24±0.02

IV. Conclusions

- The present report was intended to proof the variations of fission modes observed i Ref. [1] using the advantage of simultaneous measurement of resonance and therma neutron induced fission provided by the IBR-30 neutron source.
- Resonance neutron induced fission mode variations were observed similar to thos given in Ref [1].

- The neutron energy resolution in the present work was much worse, but the acquired statistics was at least by order of magnitude higher. Much more statistically meaningful results were obtained for resonances below 8.77 eV.

- A skewed Gaussian representation for the average TKE(A) was implemented providing a better agreement with the experimental distribution.

Finally one of the authors is very grateful to professor L.B. Pikelner for many fruitful discussions and for advise to improve the results by use of the steady state flux of IBR-30.

References

[1] F.-J. Hambsch, H.-H. Knitter, C. Budtz-Jørgensen, and J.P. Theobald, Nucl. Phys. A491, 56 (1989).
[2] Sh. S. Zeinalov, M. Florek, W.I. Furman, V.A. Kriatchkov and Yu. S. Zamyatnin, Proc. 7th Int. Seminar on Interaction of Neutrons with Nuclei (ISINN-7), Dubna, Russia, May 25-28, 1999.
[3] F.-J. Hambsch, Proc. 12th Int. Seminar on Interaction of Neutrons with Nuclei (ISINN-12), Dubna, Russia, May 26-29, 2004.
[4] O. Bunemann, T.E. Granshaw, and J.A. Harvey, Can. Jour. Res. A27 (1949) 191.
[5] A. Oed, P. Geltenbort, F. Gönnenwein, T. Manning, and D. Souque, Nucl. Instr. Meth. 205 (1983) 455.
[6] C. Budtz-Jørgensen, H.-H. Knitter, Ch. Straede, F.-J. Hambsch and R. Vogt. Nucl. Instr. Meth. A285, 209 (1987).
[7] H.-H. Knitter, F.-J. Hambsch, C. Budtz-Jørgensen, Ch. Straede, Proc. of Int. Conf. on Neutron Physics, Kiev, Sept. 1987.
[8] U. Brosa, S. Grossmann, A. Müller, Phys. Rep. 197 (1990)167.
[9] U. Brosa, H.-H. Knitter, Proc. of the XVIIIth Int. Symp. On Nuclear Physics and Chemistry of Fission, Gaussig, GDR, 1988, ed. H. Marten, D. Seeliger, Xfk-732, p. 145.